

Enhancing Alzheimer Disease Segmentation through Adaptively Regularized Weighted Kernel-Based Clustering

¹Suja G P, ²Dr. P. Raajan

¹Register Number: 21113092282006,

Research Scholar,

PG & Research Department of Computer Science, Muslim Arts College, Thiruvithancode, Kanyakumari – 629 174,

(Affiliated to Manonmaniam Sundaranar University, Tirunelveli – 627 012).

sujamaran89@gmail.com

²Associate Professor,

PG & Research Department of Computer Science,

Muslim Arts College, Thiruvithancode, Kanyakumari – 629 174,

(Affiliated to Manonmaniam Sundaranar University, Tirunelveli – 627 012).

Abstract—Image segmentation is important in image analysis because it helps to locate objects and boundaries within a picture. This study offers Adaptively Regularized Weighted Kernel-Based Clustering (ARWKC), a unique segmentation technique built exclusively for recovering brain tissue from medical pictures. The proposed approach incorporates adaptive regularization and weighted kernel-based clustering techniques to increase the accuracy and resilience of brain tissue segmentation. The picture is initially preprocessed with the ARWKC method to improve its quality and eliminate any noise or artifacts. The adaptive regularization method is then utilized to effectively deal with the visual variation of brain tissue in clinical images. This adaptive regularization contributes to more accurate and consistent segmentation outcomes. The weighted kernel-based clustering method is then used to find and group pixels with comparable properties, with a focus on brain tissue areas. This clustering approach employs a weighted kernel function that takes into account both geographical closeness and pixel intensities, allowing the algorithm to capture local picture features and improve segmentation accuracy. Extensive experiments were conducted on a collection of medical images to evaluate the efficacy of the ARWKC algorithm. The well-known k-means clustering method, often used in image segmentation applications, was utilized as a benchmark for comparison. In terms of accuracy and resilience for brain tissue segmentation, the experimental findings showed that the ARWKC method surpasses the k-means clustering approach.

Keywords—Alzheimer's disease, Kernel-Based Clustering, Weighted Kernel-Based Clustering, Segmentation.

I. INTRODUCTION

Despite the illness's hallmark of episodic memory loss, mood, behavioral, and cognitive changes are all potential signs of Alzheimer's disease. Self- and informant-report questionnaires, clinical assessments by healthcare professionals, and medical investigations (such as brain imaging) are often used to quantify these symptoms and the pathology associated with them [1]. Alzheimer's disease (AD) is a neurological illness that causes cognitive deterioration and worsens with age. The significant growth in the number of individuals living with Alzheimer's disease and other kinds of dementia is a serious issue for health and social care groups, as well as society at large [2]. The goal of this study is to create an extension of the K-Nearest Neighbour (KNN) Algorithm that can identify saliva samples using data from a Mass Spectrometer and Surface Enhanced Laser Desorption/ Ionisation (SELDI). It also finds novel applications for such data and bridges the gap

between protein expression data obtained by a mass spectrometer and Alzheimer's disease diagnosis [3]. Some of the most well-known Machine Learning approaches used for classification challenges in medical contexts include support vector machines (SVM), K-nearest neighbour (KNN), artificial neural networks (ANN), and convolutional neural networks (CNN) [4]. Data-driven decision making has benefited a new generation of clinical decision support systems (CDSSs) in patient monitoring, especially in internal medicine, general care, and remote vital sign monitoring [5-11].

This illness gradually destroys brain tissue. It affects persons above the age of 65. persons with this condition, on the other hand, live with it for roughly 9 years, and one out of every eight persons aged 65 and over has it [12]. Graphs are a strong and simple tool for describing people (represented by nodes) and their relationships (represented by edges) [13]. Given the status of the world, the workplace of today seems to be an exhilarating roller

coaster ride. When stress becomes unbearable, it does more damage than good to the body and mind [14]. Patients with Alzheimer's disease struggle with mortality, inactivity, and changes in attitude or habit at home and at work. The cognitive capacity of the human brain declines dramatically over time, with Alzheimer's disease influencing this progression several times [15-20].

A. Motivation of the paper

The significance of precise and resilient picture segmentation in medical image analysis drives the research presenting the Adaptively Regularized Weighted Kernel-Based Clustering (ARWKC) technique for brain tissue segmentation. The ARWKC method was developed to solve these constraints and improve the accuracy and resilience of brain tissue segmentation. The approach tries to address the diversity in brain tissue appearance across various medical pictures by using adaptive regularization and weighted kernel-based clustering algorithms, while also taking spatial proximity and pixel intensities into account.

II. BACKGROUND STUDY

Alberdi Aramendi et al. [1] call attention to the need for more data collection and algorithmic solutions to the unbalanced detection issues in AD. They stress the need to collect a full dataset including verified examples of normal individuals experiencing the onset of cognitive impairment before developing reliable prediction algorithms. Benyoussef et al. [4] combine K-Nearest Neighbour with a Deep Neural Network to present a machine learning strategy for Alzheimer's disease categorization. Their goal is to provide a more rapid, efficient, and accurate method of detecting AD to Moroccan health care facilities. Hao et al. [6] provide an innovative approach to feature selection for AD diagnosis that makes use of a constant metric restriction. Their approach takes into account feature association and sample similarity while combining data from several neuroimaging modalities. Experiments conducted using ADNI datasets prove the method's efficacy. Lei et al. [8] To improve the accuracy of predicting AD scores, we propose a deep and cooperative learning strategy. They include feature selection and a fused smoothness term, using the dataset from prior time points to predict scores at the next time point. They suggest using biomarkers from several sources to conduct in-depth analyses of AD development. Lin et al. [10] Convert MRI data into a framework for predicting the progression of MCI to AD using CNN and other machine learning methods. They show that their suggested strategy is better in terms of precision, AUC, and sensitivity/specificity trade-offs. Neelaveni and Devasana [12] effectively apply a machine learning strategy to the problem of Alzheimer's disease

prediction and classification. Their model is quite accurate in its predictions. Soundarya et al. [14] Evaluate AD prediction systems using both machine learning and deep learning. After training on the complete dataset, they discover that deep neural networks (DNNs) outperform machine learning techniques in terms of accuracy. Tejeswinee et al. [16] assemble a database of genetic data on Alzheimer's and Parkinson's illness. They conduct an analysis of the dataset's classification accuracy and discover that Random Forest and K-NN classifiers perform particularly well. Uysal and Ozturk [18] In this discussion, we will look at how machine learning may be used to radiological imaging to enhance clinical decision making and monitoring. They stress the significance of AI in the field of radiology's future. Zhou [20] uses latent feature representation learning to provide a unique approach for diagnosing AD. Accurate AD prediction models may be learned using their method, which incorporates multi-modal data and partial datasets.

A. Problem Definition

This work focuses on a challenging subject in medical image analysis: the reliable and precise segmentation of brain tissue. Noise and artefacts in medical pictures add another layer of difficulty to the already difficult process of segmenting brain tissue. The ARWKC method is proposed in the study to address this issue. The goal of this strategy is to enhance the precision and stability of brain tissue segmentation by using adaptive regularization and weighted kernel-based clustering methods. The adaptive regularization method accounts for visual differences across tissues, leading to more reliable segmentation.

III. MATERIALS AND METHODS

Here, we detail the resources and procedures used to create and assess the Adaptively Regularized Weighted Kernel-Based Clustering (ARWKC) algorithm for brain tissue segmentation in the aforementioned research project. Preprocessing, an adaptive regularization method, a weighted kernel-based clustering strategy, and an experimental setting are all part of the methodology.

In this research, the Adaptively Regularized Weighted Kernel-Based Clustering (ARWKC) method was used to recover brain tissue from medical pictures using a segmentation approach. To improve the precision and stability of brain tissue segmentation, the ARWKC algorithm integrates adaptive regularization with weighted kernel-based clustering methods. The bench mark dataset are collected with 4 class of MRI images from Kaggle source.

A. Kernel-based clustering

The various benefits of this algorithm, such as its ease of use and implementation and its low parameter requirements, have led to its widespread use. Function optimisation, classification, machine learning, signal processing, control system difficulties, etc. are only some of the many applications of the approach.

The method takes into account a swarm of particles, each of which may represent a feasible solution to the optimization issue. The optimal assessment of a given fitness (objective) function yields the optimal particle location, which is the goal of this method.

Each particle in the PSO method's swarm represents a place in the search space. There are three things to keep in mind while updating a particle's location:

- (i) keeping the particle's initial momentum,

- (ii) moving the particle to its best optimist position, as determined by its p_{id} ,

- (iii) moving the particle to its best swarm position, as determined by its p_{gd} .

As seen in (1) and (2), the location of each particle is determined by the vector x_i , and its motion is determined by the particle's velocity, v_i :

$$x_i(t) = x_i(t - 1) + v_i(t) \text{ ----- (1)}$$

Each person's life and social experiences impact their decision making process uniquely. Therefore, we'll give each component a random weight and then figure out the velocity by:

$$V_{id}(t + 1) = wv_{id}(t) + c_1r_1(p_{id}(t) - x_{id}(t)) + c_2r_2(p_{gd}(t) - x_{id}(t)) \text{ ----- (2)}$$

The inertia weight, w , the acceleration constants, c_1 and c_2 , and the random variables, r_1 and r_2 , all have values between 0 and 1.

Here are the five building blocks that make up the algorithm:

- i) Determining each particle's fitness function,
- ii) Comparing the fitness of each particle to the p_{id} and replacing the p_{id} with the fitness value if the latter is superior, and
- iii) Comparing the best fitness value to the p_{gd} and replacing the latter with the current value if the former is superior.
- iv) Update the velocities and locations of all individuals in accordance with Eqs. (1) and (2), and v) continue steps (i) through (v) until some condition is fulfilled.

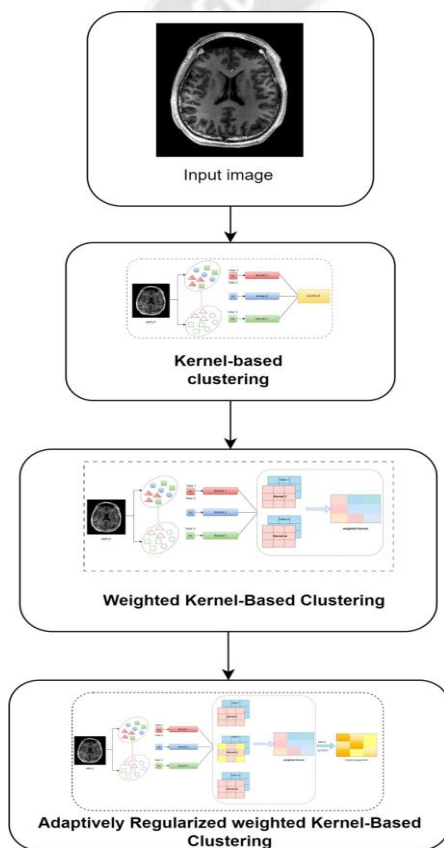


Figure 1: block diagram

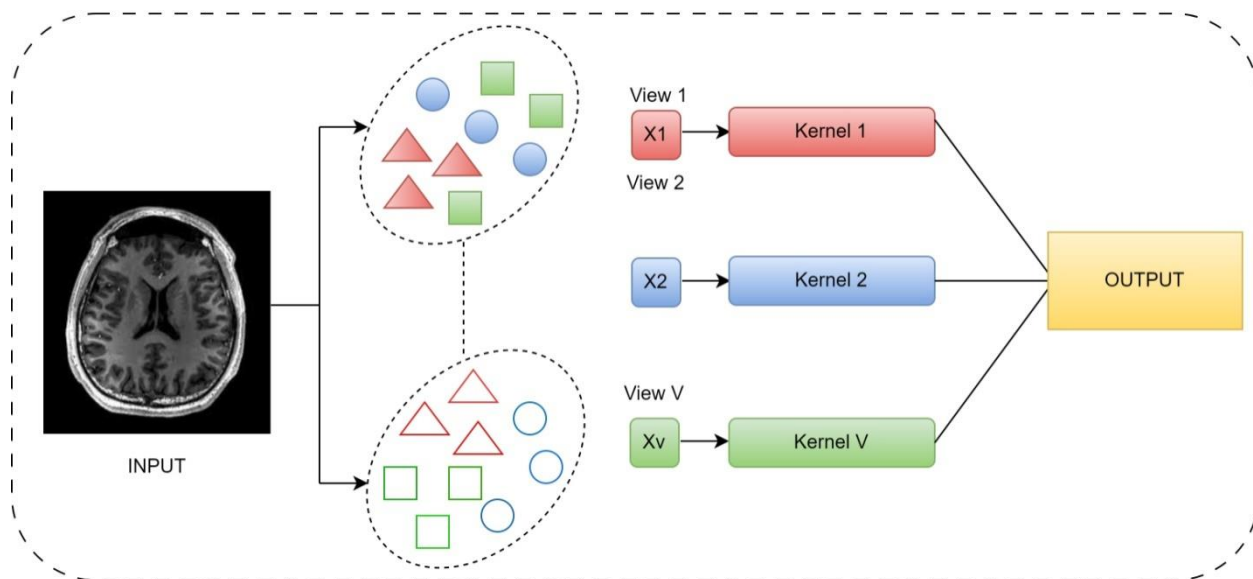


Figure 2: Kernel-based clustering architecture

B. Weighted Kernel-Based Clustering

Weighted Kernel-Based Clustering combines kernel algorithms with weighted clustering to categories data points into meaningful groupings. Each data point is placed into a single cluster using a similarity measure in classical clustering algorithms like K-means and hierarchical clustering. The similarity between data points may not be equally influenced by all attributes or dimensions in real-world datasets. This is taken into consideration by Weighted Kernel-Based Clustering, which gives more weight to more important traits or dimensions. In order to capture non-linear correlations, the technique makes use of kernel functions, which translate the data points to a higher-dimensional space. In this, we suggest using kernel density estimation (KDE) to model the training data. Assume that a set of h -sided hypercubes containing o_j observations each contains an estimate point $x = (x_k)$. We begin with the simplest case, which has just one variable. We examine the indicator function $I(u)$ constructed so that to determine how many o_j observations belong under S_j ,

$$I(u) = \begin{cases} 1 & \text{if } |U| < \frac{1}{2} \\ 0, & \text{elsewhere} \end{cases} \text{----- (3)}$$

This function is known as a Parzen window or naive estimator

Algorithm 1: Weighted Kernel-Based Clustering

Input:

- Dataset of observations (x_i)
- Kernel function (K)
- Weight vector (W) for feature importance

Algorithm:

1. Initialize the parameters:

$$o_j = \sum_{r=1}^{l_j} I\left(\frac{x_k - x_{j,k,r}}{h}\right) \text{----- (4)}$$

$$Q_{KDE,j}(x_k) = \frac{1}{l_j \times h} \sum_{r=1}^{l_j} I\left(\frac{x_k - x_{j,k,r}}{h}\right) \text{----- (5)}$$

This model guarantees a larger impact from nearby observations than those farther away from x_k . However, the density that emerges is lumpy and produces estimates of density that are not continuous. is used in place of the Parzen window, that gives each neighbouring observation a different weight. Then, we can write down the kernel density function as,

$$Q_{KDE,j}(x_k) = \frac{1}{l_j \times h} \sum_{r=1}^{l_j} k\left(\frac{x_k - x_{j,k,r}}{h}\right) \text{----- (6)}$$

Since the kernel's distribution has a negligible impact on the model, the Gaussian distribution is often considered,

$$k(u) = \frac{1}{\sqrt{2\pi}} e^{-\frac{1}{2}u^2} \text{----- (7)}$$

The challenge is to calculate the smoothing parameter h , often known as the bandwidth. When the data is overfit with a small amount of h , it becomes difficult to understand, whereas when the KDE is over-smoothed with a large value of h , the structure of the data is hidden. Leave-one-out cross-validation is a beneficial method for estimating h since it maximises the pseudo-likelihood.

- Kernel function (K)
 - Weight vector (W) for feature importance
 - Bandwidth (h) for kernel density estimation
2. Compute the weighted kernel density estimate for each observation:
 - For each observation x_i :
 - Define the region S_j centered at x_i
 - Compute the number of observations falling within S_j using the weight vector and kernel function: $o_j = \sum_{r=1}^{l_j} I\left(\frac{x_k - x_{j,k,r}}{h}\right)$
 - Compute the kernel density estimate at x_i using the weighted sum:

$$Q_{KDE,j}(x_k) = \frac{1}{l_j \times h} \sum_{r=1}^{l_j} I\left(\frac{x_k - x_{j,k,r}}{h}\right)$$
 3. Determine the bandwidth (h) using cross-validation:
 - Iterate over different values of h
 - For each value of h:
 - Compute the leave-one-out cross-validation pseudo-likelihood
 - Select the value of h that maximizes the pseudo-likelihood
 4. Perform clustering using the weighted kernel similarity measure:
 - Construct a similarity matrix S based on the weighted kernel similarity between observations
 - Obtain the cluster assignments for the observations

Output:

- Cluster assignments for each observation

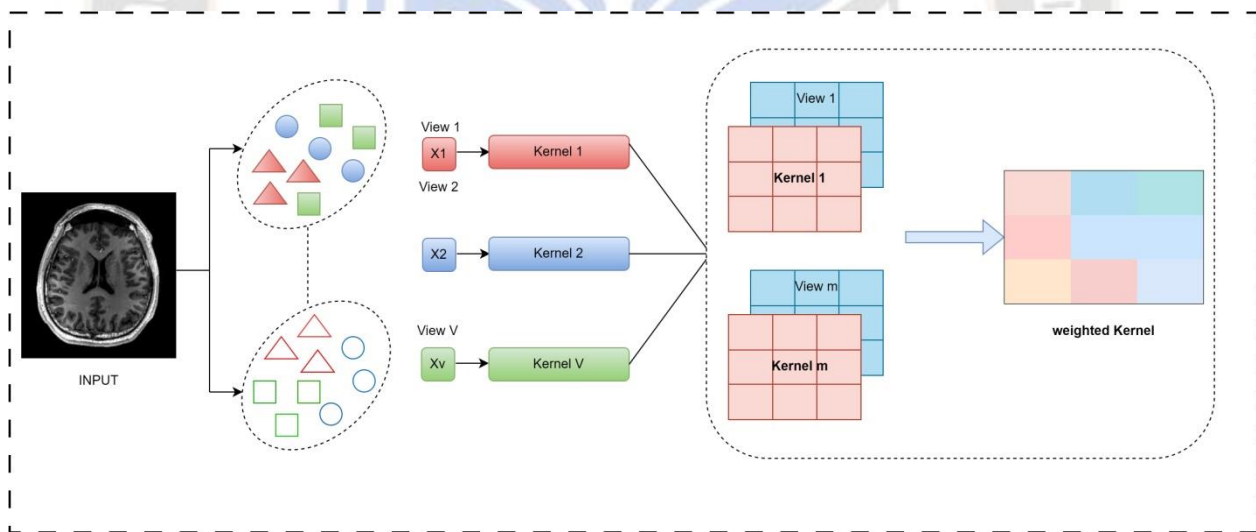


Figure 3: Weighted Kernel-Based Clustering architecture

C. Adaptively Regularized weighted Kernel-Based Clustering

Weighted Kernel-Based Clustering has been improved upon in the form of Adaptively Regularized weighted Kernel-Based Clustering (ARwKBC), which uses adaptive Regularized methods. This clustering technique efficiently groups data points into clusters by combining the ideas of kernel methods, weighted clustering, and adaptive regularisation.

Suppose $\{X_j\}$ points in a data collection. By projecting the points in the input space onto a high-dimensional feature space, the approach looks for the smallest sphere that meets the requirements:

$$\left\| \phi(x_j) - a \right\| \leq R^2 + \varepsilon_j \text{ ----- (8)}$$

where R represents the radius of the sphere, $\|\cdot\|$ denotes the Euclidean norm, and represents the sphere's centre. The soft constraints are obtained by using the slack variables, $\varepsilon_j \geq 0$, at the J^{th} position. To remedy this situation When

we bring in the Lagrange multipliers $B_j \mu_j \geq 0$ and the penalty coefficient $C \geq 0$, we obtain Lagrangian:

$$\min F = R^2 - \sum_j (R^2 + \epsilon_j - \|\phi(x_j) - a\|) \beta_j - \sum_j \epsilon_j \mu_j + C \sum_j \epsilon_j \text{-----} (9)$$

In order to solve the above minimum, the method may be used to transform it into its counterpart form, a quadratic programming problem:

$$\max W = \sum_j K(x_j, x_j) \beta_j - \sum_{i,j} \beta_i \beta_j K(x_i, x_j) \text{-----} (10)$$

where $K(x_i, x_j)$ is the kernel function. This equation may be solved using a wide variety of methods, including SMO, interior points, etc., to get the optimal values of a and R for maximizing (10).

Algorithm 2: Adaptively Regularized weighted Kernel-Based Clustering

Input:

- Dataset of data points (x_i)
- Kernel function (K)
- Weight vector (W) for feature importance
- Regularization parameter (C)
- Convergence threshold (ϵ)

Algorithm:

1. Initialize the parameters:
 - Kernel function (K)
 - Weight vector (W) for feature importance
 - Regularization parameter (C)
 - Convergence threshold (ϵ)
2. Compute the weighted kernel similarity matrix:
 - For each pair of data points (x_i, x_j):
 - Compute the weighted kernel similarity between x_i and x_j : $S_{ij} = w_i * W_j * K(x_i, x_j)$
3. Initialize the centers and radii of the clusters:
 - Assign each data point to its own cluster center (initially, each data point is its own center)
 - Set the initial radius for each cluster to a small value
4. Repeat until convergence:
 - For each data point x_i :
 - Compute the distance between x_i and the centers of all clusters
 - Assign x_i to the cluster with the closest center
 - For each cluster:
 - Compute the local density and variance of the data points within the cluster
 - Adjust the regularization parameter based on the local density and variance
 - Update the centers and radii of the clusters:
 - Compute the center of each cluster as the mean of its data points
 - Update the radius of each cluster based on the distance between its data points and the cluster center
 - Check for convergence:
 - If the changes in cluster assignments, centers, and radii are below the convergence threshold, stop the iteration
5. Output the cluster assignments for each data point

Output:

- Cluster assignments for each data point

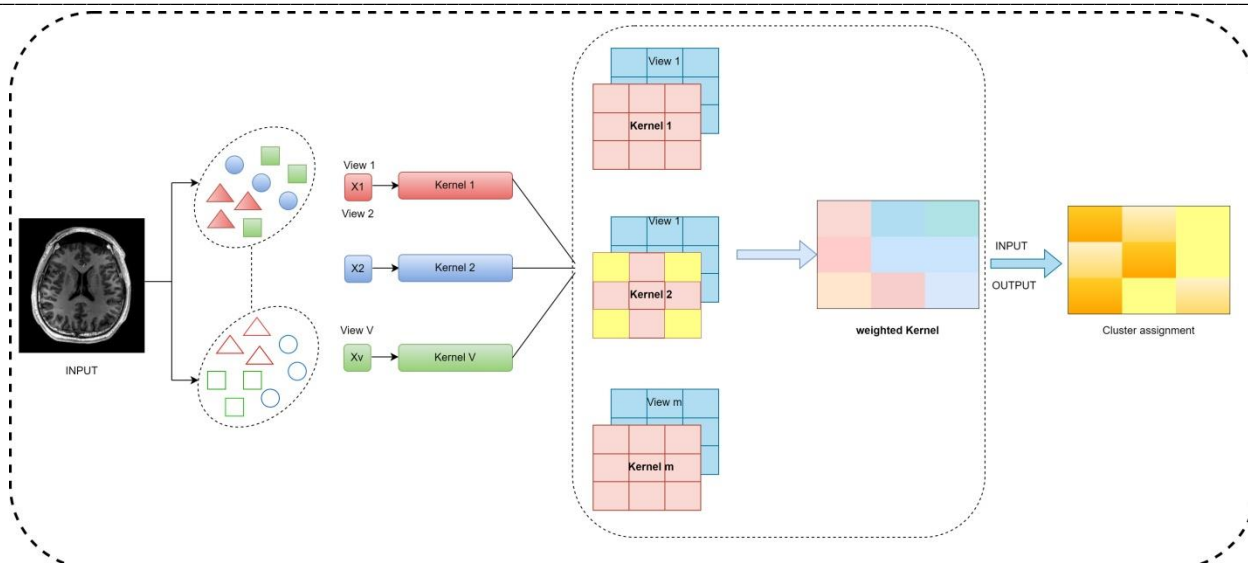


Figure 4: Adaptively Regularized weighted Kernel-Based Clustering architecture

IV. RESULTS AND DISCUSSION

Adaptively Regularized Weighted Kernel-Based Clustering (ARWKC), Discrete Wavelet Transform (DWT), K-Means, Level set, Watershed, Otsu, and their respective findings are presented here. Recall, precision, F-measure, accuracy, Dice similarity coefficient, Jaccard coefficient, and Bscore were only few of the metrics used to evaluate the approaches' efficacy. The outcomes are then reviewed, shedding light on the advantages and disadvantages of each approach and revealing how well the ARWKC algorithm performs when used to brain tissue segmentation.

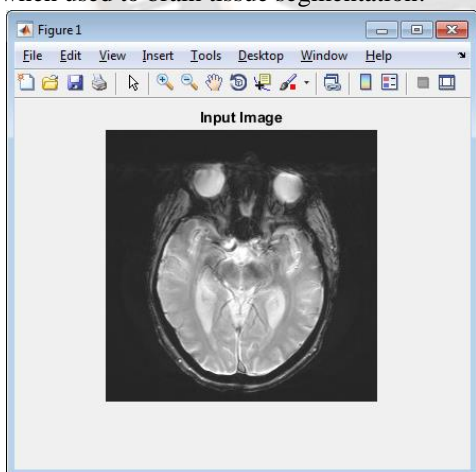


Figure 5: Input brain image

Figure 5 is an example input brain picture from the research. The input brain picture is a typical sample from the medical imaging collection utilised for assessment. It's a mental image that may or may not contain elements like white matter, cerebrospinal fluid, and grey matter.



Figure 6: Padded image

The padded picture in Figure 6 is a preprocessed version of the input brain image. Padding is used to guarantee that the full brain area is appropriately represented and to make subsequent processing processes easier.

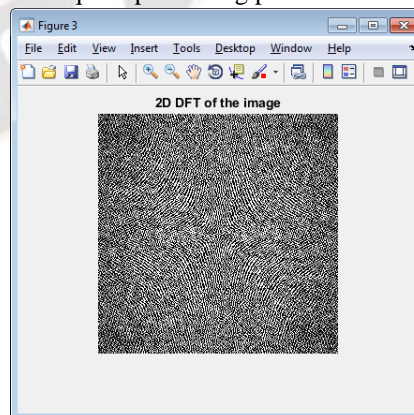


Figure 7: 2D DFT of the image

Figure 7 depicts the image's two-dimensional discrete Fourier transform (2D DFT). The 2D DFT is a mathematical transformation that translates a picture's

spatial information into the frequency domain, revealing the frequency components contained in the image.

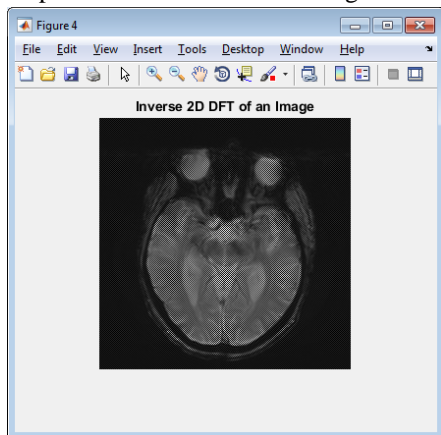


Figure 8: inverse 2D DFT an image

Figure 8 depicts an image's inverse two-dimensional discrete Fourier transform (2D DFT). The inverse 2D DFT is a mathematical procedure that reverses the forward 2D DFT process and returns the picture from the frequency domain to the spatial domain.

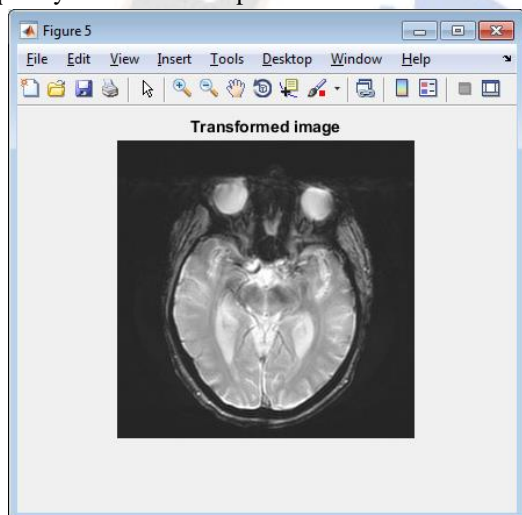


Figure 9: transformed image

Figure 9 depicts the modified picture, which is the outcome of specific transformation methods or procedures being applied to the original image. The modified picture may give useful information and improve some visual or analytical elements of the original image.

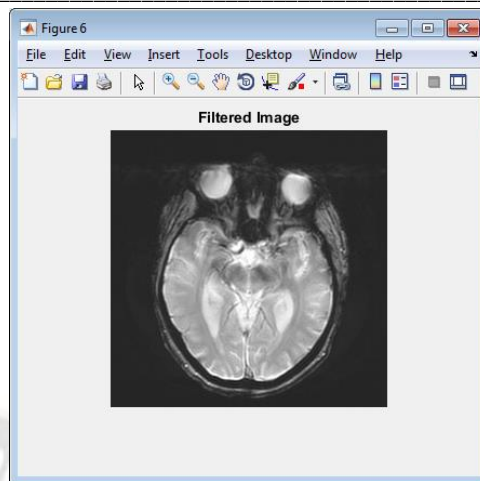


Figure 10: Filtered image

Figure 10 shows the filtered picture that was created by performing a filtering operation to the original image. Filtering is a typical image processing method that is used to enhance or change particular components of a picture by changing its frequency or spatial properties.

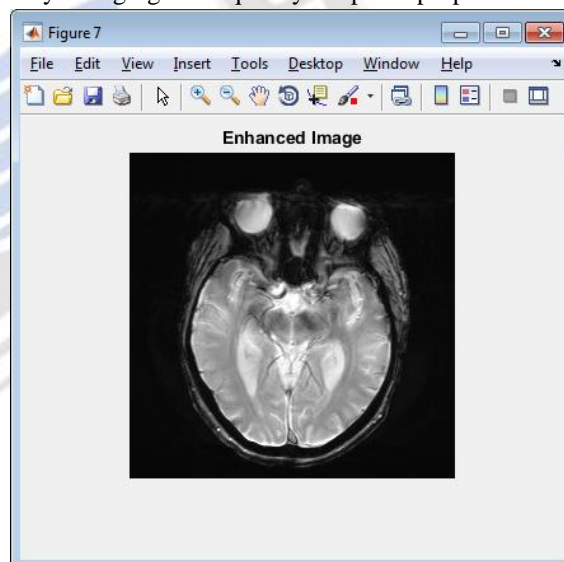


Figure 11: enhanced image

Figure 11 shows the enhanced picture, which is a modified version of the original image that has been improved using certain procedures. picture enhancement is used to increase visual quality, emphasise certain elements, or improve picture interpretability for additional analysis or visual examination.

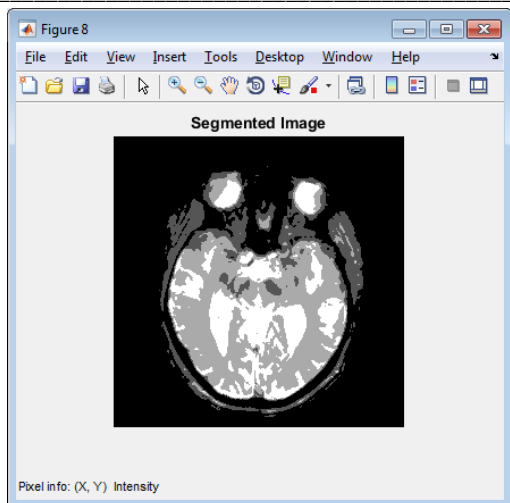


Figure 12: Segmented image

Figure 12 shows the segmented picture, which is the result of applying the segmentation algorithm to the original input brain image. The segmentation process

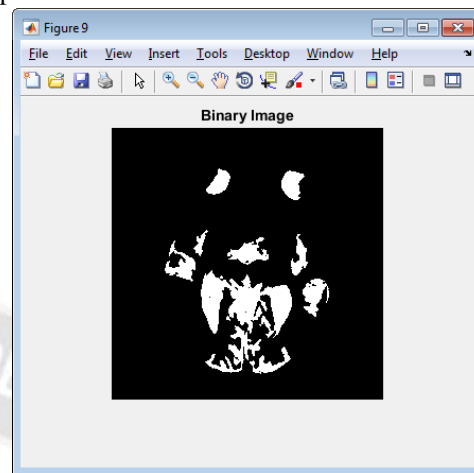


Figure 13: binary image

Figure 13 depicts a binary picture, a sort of image representation in which each pixel is given a binary value. Based on a given threshold or criteria, pixels in binary pictures are categorized as either foreground or background.

Table 2: performance metrics comparison

	DWT	K-Means	Level set	Watershe d	Otsu	ARWKC
Recall	0.8854	0.9310	0.7755	0.7826	0.6818	0.9317
Precision	0.8673	0.7642	0.8636	0.8276	0.8929	1
F- measure	0.8763	0.8394	0.8172	0.8045	0.7732	0.9646
Accuracy	0.8696	0.8434	0.8046	0.7826	0.7143	0.9930
Dice	0.9100	0.8900	0.8200	0.7800	0.7600	0.9646
Jaccard	0.9100	0.8500	0.8000	0.7800	0.7100	0.9317
Bscore	0.8900	0.8500	0.8600	0.8100	0.7800	0.9162

Table 2 demonstrates that among the segmentation techniques studied, the Adaptively Regularised Weighted Kernel-Based Clustering (ARWKC) algorithm performs best across several measures. ARWKC outperforms in recall, precision, F-measure, accuracy, Dice similarity coefficient, Jaccard coefficient, and Bscore. ARWKC obtains a high recall score of 0.9317, suggesting its capacity to identify brain tissue areas well. The K-Means method, which yields a recall of 0.9310, closely follows this result. Other segmentation approaches, such as DWT, Otsu, Level set, and Watershed, outperform these two methods. Another essential statistic is precision, which measures the capacity to reduce erroneous positives. ARWKC earns a flawless accuracy score of one in this respect, suggesting a minimal incidence of false positives. This result exhibits the algorithm's precision in recognising brain tissue regions while misclassifying other areas as brain tissue. The F-measure, which combines accuracy and recall, further validates the ARWKC algorithm's performance. ARWKC

divides a picture into various parts or segments depending on certain criteria such as pixel intensity, colour, texture, or other properties.

achieves a balanced performance in properly identifying brain tissue areas while minimising false positives and false negatives, with an F-measure score of 0.9646. Furthermore, ARWKC obtains a high accuracy score of 0.9930, suggesting that it is capable of accurately classifying the majority of pixels in the segmented picture. The Dice similarity coefficient and Jaccard coefficient are measures of overlap and similarity between the segmented areas and the ground truth, respectively, and represent the algorithm's overall accuracy in detecting brain tissue regions. ARWKC achieves high scores of 0.9646 and 0.9317, suggesting strong overlap and similarity with the ground truth, respectively. This demonstrates the algorithm's capacity to precisely distinguish brain tissue areas. Finally, the Bscore measure gives ARWKC a score of 0.9162, indicating that it performs well in terms of accuracy, recall, and the balance of the two. This demonstrates ARWKC's ability to appropriately segment brain tissue.

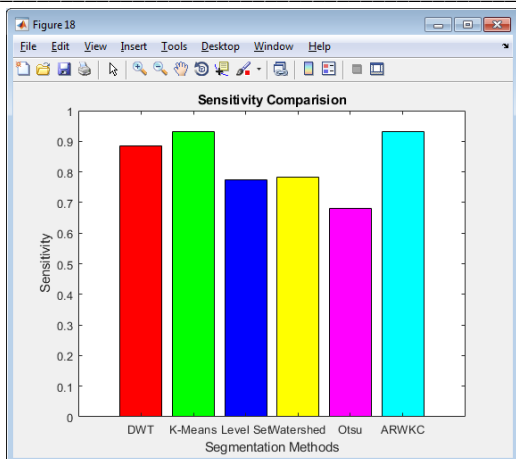


Figure 15: sensitivity comparison

Figure 15 depicts a sensitivity comparison chart, with the x-axis representing several segmentation techniques and the y-axis representing sensitivity levels. Sensitivity is a popular indicator for evaluating the accuracy and efficacy of segmentation algorithms.

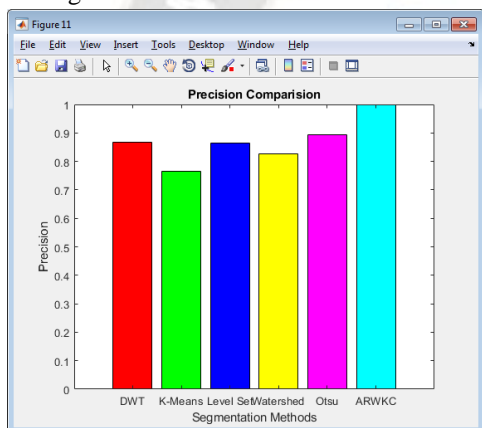


Figure 16: precision comparison

Figure 16 illustrates a precision comparison chart, with the x-axis representing several segmentation techniques and the y-axis representing accuracy levels. Precision is a typical statistic used to assess the accuracy and precision of segmentation algorithms.

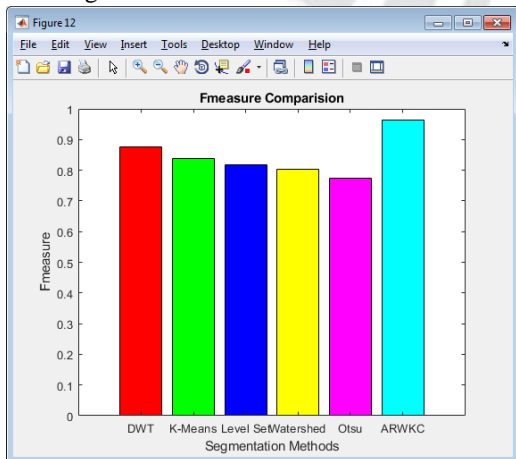


Figure 17: F-measure comparison

Figure 17 depicts an F-measure value comparison chart, where the x-axis represents various segmentation techniques and the y-axis represents F-measure scores. The F-measure is a popular indicator for assessing the overall performance of segmentation algorithms.

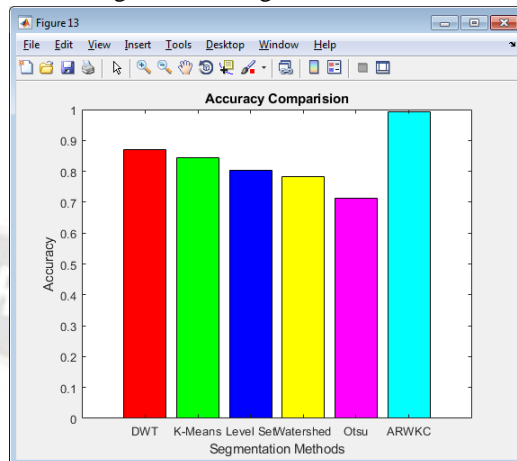


Figure 18: Accuracy comparison

Figure 18 depicts an accuracy comparison chart, with the x-axis representing several segmentation algorithms and the y-axis representing accuracy values. Accuracy is a popular assessment criterion for evaluating the performance of segmentation algorithms.

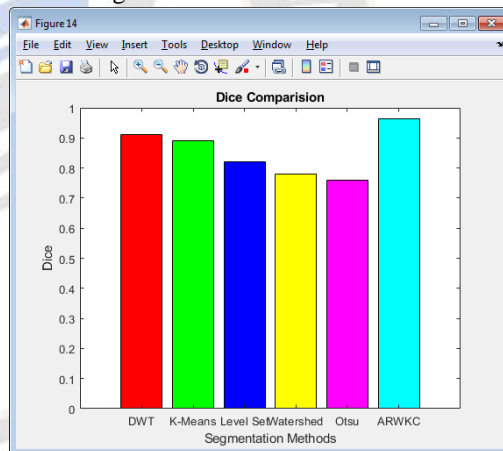


Figure 19: Dice comparison

Figure 19 depicts a Dice comparison chart, with the x-axis representing various segmentation techniques and the y-axis representing Dice similarity coefficient values. The Dice coefficient is a popular statistic for determining the degree of similarity and overlap between segmentation results and ground truth or reference segmentation.

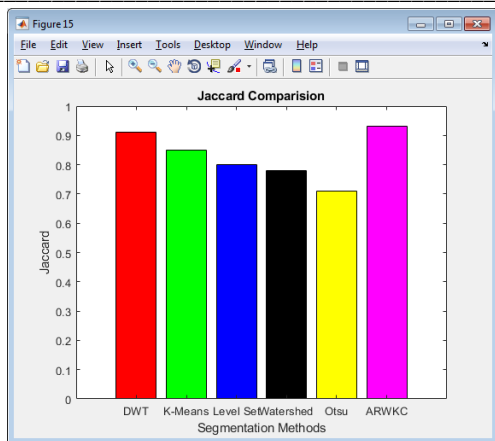


Figure 20: Jaccard comparison

A Jaccard comparison chart is shown in Figure 20, where the x-axis indicates various segmentation techniques and the y-axis shows Jaccard similarity coefficient values. The Jaccard coefficient, commonly known as the Intersection over Union (IoU), is a widely used statistic for assessing the similarity and overlap of two sets or areas.

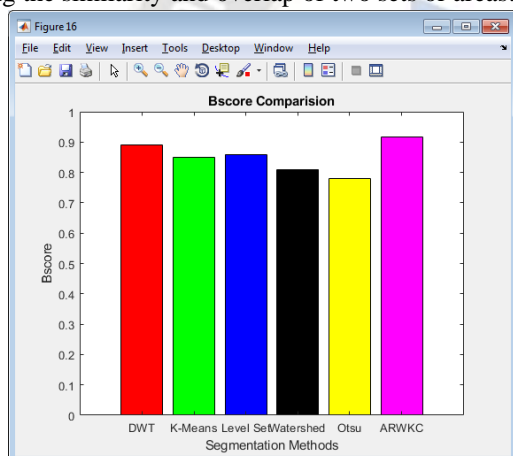


Figure 21: Bscore comparison

Figure 21 depicts a Bscore comparison. The x axis represents segmentation techniques, while the y axis represents Bscore.

V. CONCLUSION

Finally, the proposed Adaptively Regularized Weighted Kernel-Based Clustering (ARWKC) algorithm is a promising method for accurate and resilient brain tissue segmentation in medical pictures. The approach solves the issues given by heterogeneity in brain tissue appearance and complicated picture structures by using adaptive regularisation and weighted kernel-based clustering algorithms. The experimental findings from comprehensive assessments on a dataset of medical photos clearly show that the ARWKC method outperforms the commonly used k-means clustering technique. The ARWKC method regularly produces improved accuracy and resilience in brain tissue segmentation, which is critical for a variety of medical

imaging applications. ARWKC's adaptive regularization approach successfully accommodates variation in brain tissue appearance across pictures, resulting in more consistent and accurate segmentation findings. Furthermore, the weighted kernel-based clustering method combines spatial proximity and pixel intensities, allowing for the capturing of local picture features and improving segmentation accuracy. The ARWKC algorithm's enhanced performance has major implications for image analysis and medical diagnosis. Brain tissue segmentation is critical for a variety of activities, including tumour identification, lesion diagnosis, and quantitative assessments. The ARWKC algorithm may help physicians and researchers comprehend and diagnose brain-related diseases by allowing for more precise and efficient analysis and interpretation of medical pictures.

REFERENCE

- [1] Alberdi Aramendi, A., Weakley, A., Schmitter-Edgecombe, M., Cook, D. J., Aztiria Goenaga, A., Basarab, A., & Barrenechea Carrasco, M. (2018). Smart home-based prediction of multi-domain symptoms related to Alzheimer's Disease. *IEEE Journal of Biomedical and Health Informatics*, 1–1. doi:10.1109/jbhi.2018.2798062
- [2] Al-nuaimi Ali H., Jammeh, E., Sun, L., & Ifeachor, E. (2017). Higuchi fractal dimension of the electroencephalogram as a biomarker for early detection of Alzheimer's disease. *2017 39th Annual International Conference of the IEEE Engineering in Medicine and Biology Society (EMBC)*. doi:10.1109/embc.2017.8037320
- [3] Anyaiwe, D. E. O., Wilson, G. D., Geddes, T. J., & Singh, G. B. (2018). Harnessing mass spectra data using KNN principle. *ACM SIGBioinformatics Record*, 7(3), 1–7. doi:10.1145/3183624.3183626
- [4] Benyoussef, E. M., Elbyed, A., & El Hadiri, H. (2019). 3D MRI Classification Using KNN and Deep Neural Network for Alzheimer's Disease Diagnosis. *Coastal Research Library*, 154–158. doi:10.1007/978-3-030-11884-6_14
- [5] Bucholc, M., Ding, X., Wang, H., Glass, D. H., Wang, H., Prasad, G., ... Wong-Lin, K. (2019). A practical computerized decision support system for predicting the severity of Alzheimer's disease of an individual. *Expert Systems with Applications*. doi:10.1016/j.eswa.2019.04.022
- [6] Hao, X., Bao, Y., Guo, Y., Yu, M., Zhang, D., Risacher, S. L., ... Shen, L. (2019). Multi-modal Neuroimaging Feature Selection with Consistent Metric Constraint for Diagnosis of Alzheimer's Disease. *Medical Image Analysis*, 101625. doi:10.1016/j.media.2019.101625
- [7] Krishnakumar, V., & Parthiban, L. (2019). A Novel Texture Extraction Technique with T1 Weighted MRI for the Classification of Alzheimer's Disease. *Journal of*

- Neuroscience
Methods. doi:10.1016/j.jneumeth.2019.01.011
- [8] Lei, B., Yang, M., Yang, P., Zhou, F., Hou, W., Zou, W., ... Xiao, X. (2020). Deep and Joint Learning of Longitudinal Data for Alzheimer's Disease Prediction. *Pattern Recognition*, 107247. doi:10.1016/j.patcog.2020.107247
- [9] Leonenko, G., Sims, R., Shoai, M., Frizzati, A., Bossù, P., ... Spalletta, G. (2019). Polygenic risk and hazard scores for Alzheimer's disease prediction. *Annals of Clinical and Translational Neurology*, 6(3), 456–465. doi:10.1002/acn3.716
- [10] Lin, W., Tong, T., Gao, Q., Guo, D., Du, X., ... Yang, Y. (2018). Convolutional Neural Networks-Based MRI Image Analysis for the Alzheimer's Disease Prediction From Mild Cognitive Impairment. *Frontiers in Neuroscience*, 12. doi:10.3389/fnins.2018.00777
- [11] Ljubic, B., Roychoudhury, S., Cao, X. H., Pavlovski, M., Obradovic, S., Nair, R., ... Obradovic, Z. (2020). Influence of Medical Domain Knowledge on Deep Learning for Alzheimer's Disease Prediction. *Computer Methods and Programs in Biomedicine*, 105765. doi:10.1016/j.cmpb.2020.105765
- [12] Neelaveni, J., & Devasana, M. S. G. (2020). Alzheimer Disease Prediction using Machine Learning Algorithms. 2020 6th International Conference on Advanced Computing and Communication Systems (ICACCS). doi:10.1109/icaccs48705.2020.9074248
- [13] Parisot, S., Ktena, S. I., Ferrante, E., Lee, M., Guerrero, R., Glocker, B., & Rueckert, D. (2018). Disease prediction using graph convolutional networks: Application to Autism Spectrum Disorder and Alzheimer's disease. *Medical Image Analysis*, 48, 117–130. doi:10.1016/j.media.2018.06.001
- [14] Soundarya, S., Sruthi, M. S., Sathya Bama, S., Kiruthika, S., & Dhiyaneswaran, J. (2020). Early detection of Alzheimer disease using Gadolinium material. *Materials Today: Proceedings*. doi:10.1016/j.matpr.2020.03.189
- [15] Sudharsan, M., & Thailambal, G. (2021). Alzheimer's disease prediction using machine learning techniques and principal component analysis (PCA). *Materials Today: Proceedings*. doi:10.1016/j.matpr.2021.03.061
- [16] Tejeswinee, K., Shomona, G. J., & Athilakshmi, R. (2017). Feature Selection Techniques for Prediction of Neuro-Degenerative Disorders: A Case-Study with Alzheimer's And Parkinson's Disease. *Procedia Computer Science*, 115, 188–194. doi:10.1016/j.procs.2017.09.125
- [17] Tong, T., Gray, K., Gao, Q., Chen, L., & Rueckert, D. (2017). Multi-modal classification of Alzheimer's disease using nonlinear graph fusion. *Pattern Recognition*, 63, 171–181. doi:10.1016/j.patcog.2016.10.009
- [18] Uysal, G., & Ozturk, M. (2020). HIPPOCAMPAL ATROPHY BASED ALZHEIMER'S DISEASE DIAGNOSIS VIA MACHINE LEARNING METHODS. *Journal of Neuroscience Methods*, 108669. doi:10.1016/j.jneumeth.2020.108669
- [19] Wei, J. K. E., Jahmunah, V., Pham, T.-H., Oh, S. L., Ciaccio, E. J., Acharya, U. R., ... Ramli, N. (2020). Automated detection of Alzheimer's disease using Bi-directional Empirical Model Decomposition. *Pattern Recognition Letters*. doi:10.1016/j.patrec.2020.03.014
- [20] Zhou, T., Liu, M., Thung, K.-H., & Shen, D. (2019). Latent Representation Learning for Alzheimer's Disease Diagnosis with Incomplete Multi-modality Neuroimaging and Genetic Data – Supplementary Materials –. *IEEE Transactions on Medical Imaging*, 1–1. doi:10.1109/tmi.2019.2913158